Variations in Posture Among Average Sized Female Riders on a Touring Motorcycle

Report 2025:01, Version 1.0

Main Author

Linus Lundin

Co-authors and Reviewer(s) of the report

Maria Oikonomou, Mats Y. Svensson, Johan Iraeus

Funding

This study was funded by Strategic Vehicle Research and Innovation (FFI) (Award number: 2020-05153), by VINNOVA, the Swedish Transport Administration, Swedish Energy Agency, and industrial partners. Partners in the research project are Autoliv, BETA CAE Systems, and MIPS. This work has been carried out in association with SAFER – Vehicle and Traffic Safety Centre at Chalmers, Gothenburg, Sweden.

DEPARTMENT OF MECHANICS AND MARITIME SCIENCES
CHALMERS UNIVERSITY OF TECHNOLOGY

REPORT 2025:01
Gothenburg, Sweden, March 2025
www.chalmers.se

Contents

1. Introduction

Powered two- and three-wheelers (PTWs), such as motorcycles (MCs), are an increasingly popular mode of transportation, now accounting for 12% of the global motor vehicle fleet (WHO, 2023). However, PTW riders face a substantially higher risk of injury or fatality in crashes, making them the most vulnerable road user group worldwide (WHO, 2023).

Passive safety systems have shown promise in enhancing PTW rider safety (Ariffin et al., 2016; Capitani et al., 2010; Maier & Fehr, 2023). However, for these systems to be effective, the variability of PTW crashes must be addressed (Barbani et al., 2014; ISO 13232-6 2005; Rogers & Zellner, 2001). An important factor contributing to this variability is rider posture, which has been shown to influence injury outcomes, particularly for the two most frequently injured (AIS2+) body regions—the head and chest (Langwieder, 1977; Schaper & Grandel, 1985; Sporner et al., 1990; Wisch et al., 2019).

Despite its impact on injury risk, rider posture is often simplified in PTW safety research. Surrogates used in safety assessments, such as physical and virtual anthropometric test devices (ATDs) or finite element human body models (FE-HBMs), are typically positioned in a single rider posture (Capitani et al., 2010; ISO 13232-6 2005; Maier et al., 2021; Maier et al., 2022; Prochowski & Pusty, 2013). This approach assumes that posture is primarily dictated by the ergonomic relationship between the handlebar, seat, and foot supports—the so-called “ergonomic triangle” (Arunachalam et al., 2019; Sabbah & Bubb, 2008)—rather than individual rider preferences (Claflin, 2002; Lundin et al., 2024).

Although studies on rider posture have been conducted (Arunachalam et al., 2019; Chou & Hsiao, 2005; Robertson & Minter, 1996; Sabbah & Bubb, 2008), one of the main challenges in incorporating posture variability into PTW safety research is the lack of detailed data necessary for accurate positioning of human surrogates. Existing studies, often focused on ergonomics, typically report only average postures, usually based on mean joint angles, with occasional inclusion of standard deviations or ranges for individual joints (Barone & Curcio, 2004; Chou & Hsiao, 2005; Sabbah & Bubb, 2008; Smith et al., 2006; Van Auken et al., 2005). However, this segmented approach does not capture the full range of whole-body posture variability, which is particularly pronounced among female riders (Sabbah & Bubb, 2008).

In a previous study by Lundin et al. (2024), average and subpopulation posture variability data were compiled for 50th percentile male riders to support PTW safety system assessments. Building on these findings, the present study aims to take the first step in describing whole-body posture variability specific to 50th percentile female PTW riders. This study will provide ready-to-use posture information for positioning human surrogates in PTW crash analysis. Additionally, by comparing 50th percentile female and male postures on the same MC, this study will explore potential differences that may justify expanding future research to consider a broader range of anthropometries when assessing rider posture.

2. Method

This study follows the methodology described in Lundin et al. (2024), with the primary difference being that the previous study analyzed postures from 20 male volunteers across three different PTWs, while this current study is limited to one of these PTWs—the BMW R 1200 RT (model year 2008)—to analyze female rider postures. The following sections describe the female-specific aspects of the experimental setup.

2.1 Experimental data collection

Ten female volunteers with prior riding experience participated in the study. Their heights ranged from 157.6–168.5 cm, and their weights from 56.1–67.3 kg, with mean±SD values of 163.0±3.4 cm and 60.9±3.8 kg, respectively (Appendix A). These values are close to the 50th percentile female: 162 cm in height and 62 kg in weight (Schneider et al., 1983).

Fifty-one reflective markers were placed on anatomical landmarks, identified through palpation (Figure 1). Each volunteer was measured in three postures: (1) standing, (2) sitting on a stool, and (3) their preferred riding posture on a 2008 BMW R 1200 RT touring MC (Figure 2). The standing and sitting postures were recorded in a separate session from the riding posture.

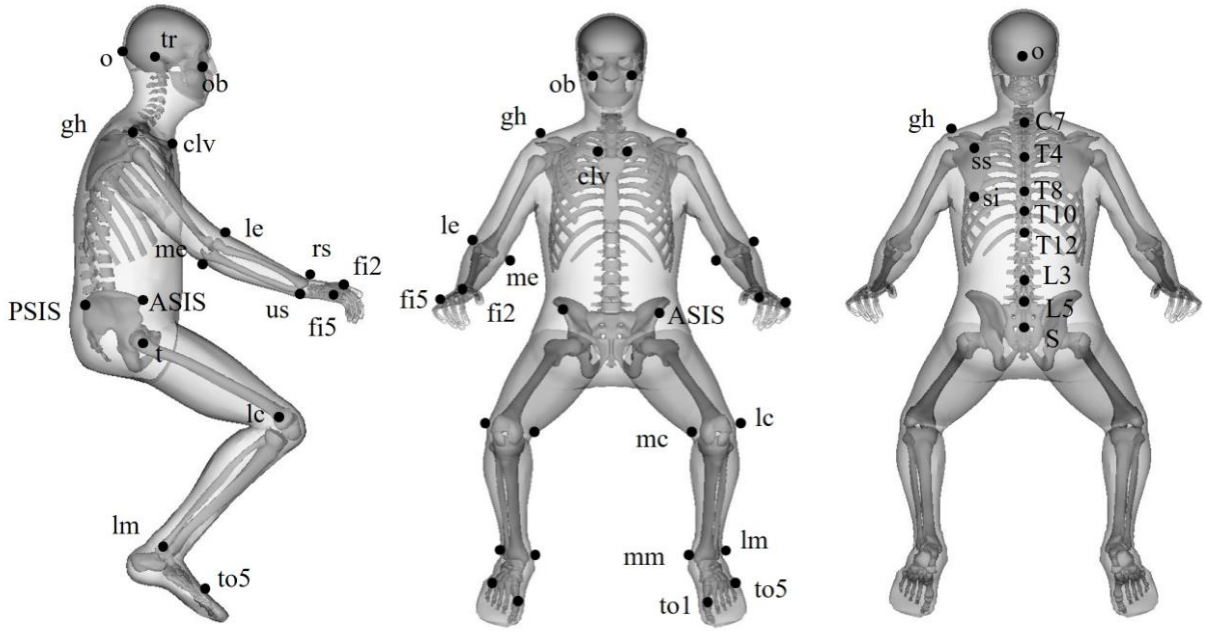

Figure 1. Illustration of marker placement on volunteers in a powered two-wheeler (PTW) rider posture. Reprinted from Lundin et al. (2024).

Figure 2. Volunteer seated on the touring motorcycle (MC), with the vehicle covered to prevent measurement interference.

2.2 Principal component analysis

Principal Component Analysis (PCA) was performed using the *pca* routine in the MATLAB Statistics and Machine Learning Toolbox (*MATLAB Statistics and Machine Learning Toolbox*, 2023) which employ single-value decomposition (SVD) with mean-centering. Based on the 3D measurements of the 10 (n) volunteers, an average posture and principal components (PCs) that capture posture variability were computed.

The standard deviation (SD) of observations' scores across PCs (σ_i) was computed. Sample volunteer postures were then derived for different SD levels using the following parametric expression:

$$sample\ volunteer\ posture\ k = \boldsymbol{\mu} + k\sigma_i \boldsymbol{l_i}, \qquad 1 \le i \le n\text{-}1 \qquad (1)$$

where $\boldsymbol{\mu}$ represents the average posture coordinates, k is the number of SD (of σ_i), $\boldsymbol{l}_i$ is the loading of the ith PC. For example, choosing k=±2 and i=1 will yield two sample (extreme) postures corresponding to ±2 SD for PC1, assuming that the variability along each PC follows a normal distribution.

A kinematic linkage model was constructed to translate the 3D marker data into an interpretable posture, defining joints using medial/lateral markers and established methods as outlined in Lundin et al. (2024) (Figure 3).

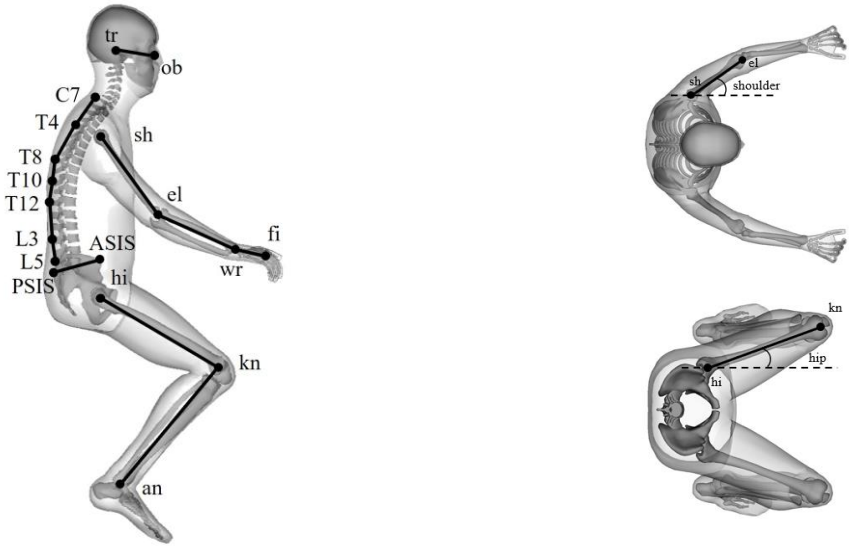

a) Mid-sagittal view b) Horizontal view

Figure 3. Kinematic linkage model created by connecting anatomical markers and joint positions. Reprinted from Lundin et al. (2024)

2.3 Outlier removal

To minimize outlier effects while retaining natural posture variance, an outlier removal process was applied based on 67 bone-to-bone distances. For each volunteer, the mean and standard deviation (SD) of each distance were calculated across three postures and three measurement repetitions.

Following the methodology of Lundin et al. (2024), a metric called the Mean Average Difference (MAD) was derived to quantify how the PCs representing posture variation changed as an increasing number of marker repetitions were identified and removed based on SD thresholds. As shown in Equation 2, the Euclidean distance was computed for each of the 51 marker positions (k=51) between the baseline data (a) and the data with removed marker repetitions (b), corresponding to the +2 SD postures for each PC. The total MAD was then obtained by averaging the Euclidean distances across all (n-1) PCs.

$$\text{MAD}^{\text{PC}} = \frac{\sum_{i=1}^{k} \|b_i - a_i\|}{k}, k = 51 \quad (2)$$

A SD threshold of 2.5 was chosen, leading to the removal of 0.4% of all marker repetitions. This threshold was selected as the least restrictive level where stricter thresholds had minimal influence on PC-derived postures, as evidenced by the relatively small changes in the total MAD value for SD levels below 2.5 (Figure 4).

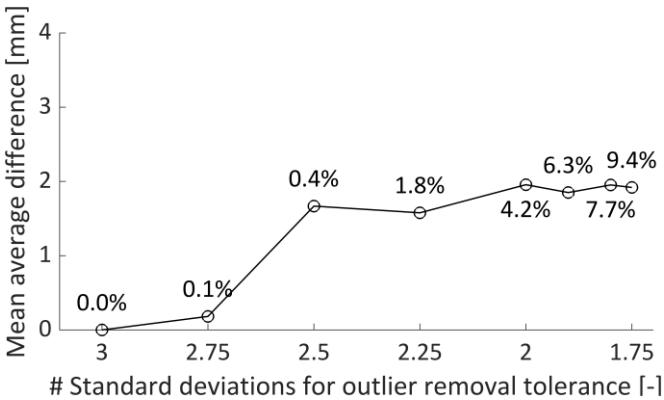

Figure 4. Total mean average difference (MAD) across various datasets with progressively stricter thresholds for removing marker repetitions. The percentage of eliminated marker repetitions is indicated above each data point.

2.4 Confidence intervals

Given the unequal sample sizes (female: n=10, male: n=20) and differences in variance, Welch's independent two-sample t-test was used to assess statistically significant differences ($p<0.05$) between characteristic angles. For joints with both left and right instances (e.g., elbow, knee), the average of both sides was calculated and used for comparison. All statistical analyses were performed using the *ttest2* function in the *MATLAB Statistics and Machine Learning Toolbox* (2023).

3. Results

The results are divided into two parts: (1) female posture analysis, and (2) a comparison between female and male postures (with data from Lundin et al. (2024).

3.1 Female analysis

The PCA identified nine PCs, with the first four cumulatively explaining over 80% of total posture variability (Figure 5). The average posture of the 10 female volunteers is visualized in Figure 6, with corresponding characteristic angles detailed in Appendix C.

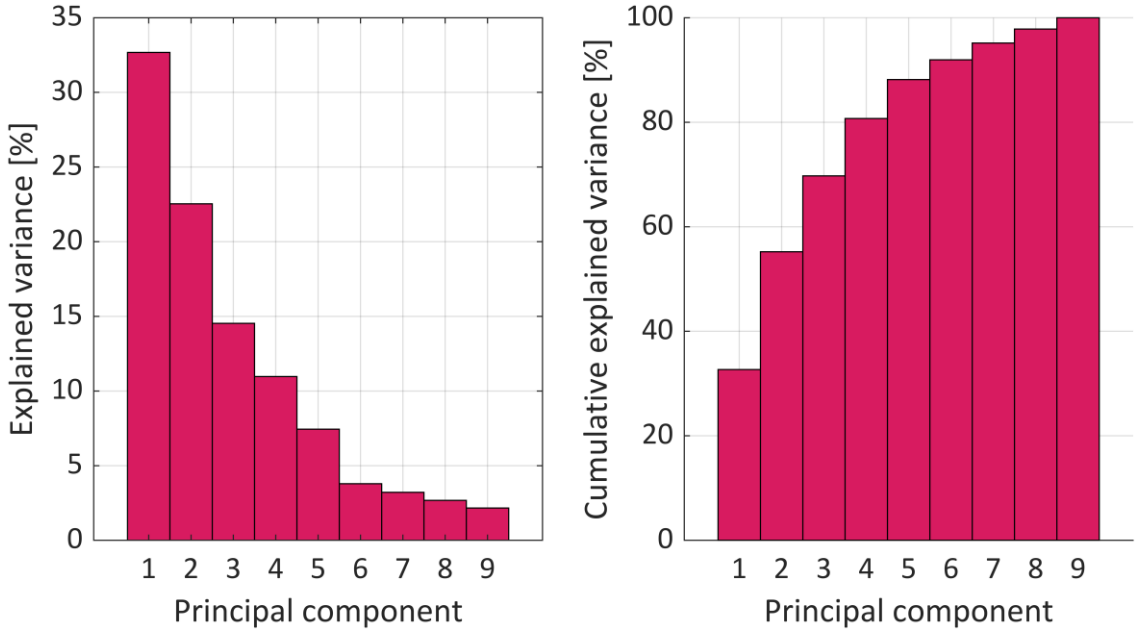

Figure 5. Scree plot showing the explained variance across principal components (left) and the cumulative explained variance (right).

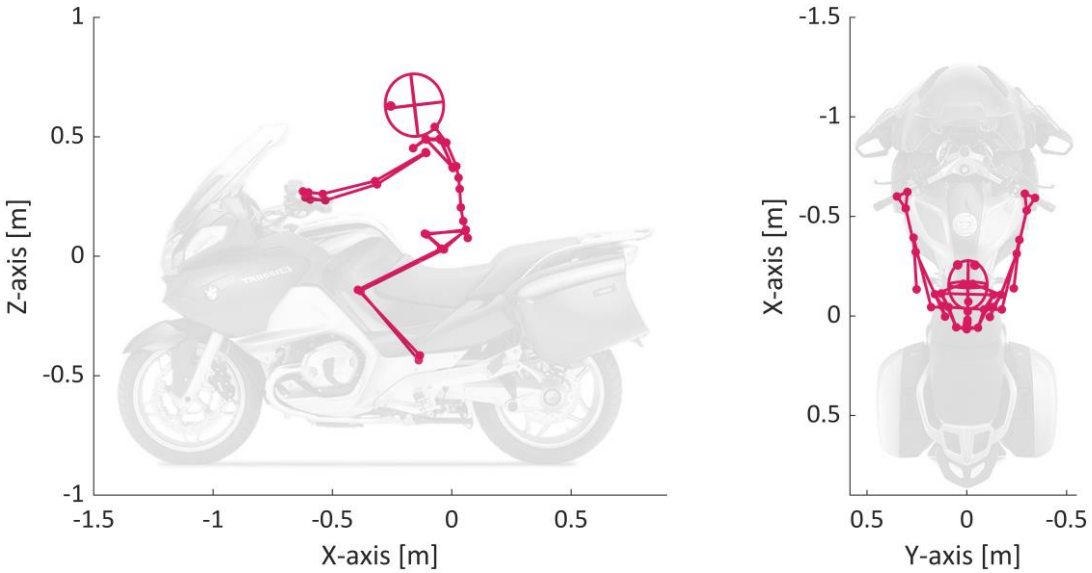

a) Mid-sagittal view b) Horizontal view

Figure 6. Average female rider posture. Note: In this Figure, posture vs. PTW comparisons are unreliable due to non-comparable suspension travel and possible distortion effects. Background photo ©BMW Motorrad.

The analysis of PCs revealed distinguishable variations in rider posture relative to the average posture, capturing different aspects of posture changes and positions on the MC. The four main PCs, which together account for 81% of the total variance, highlight distinct patterns of variability in seat position, spinal curvature, scapular movement, pelvic tilt, and asymmetry. Below is a summary of the primary posture variations identified for the first four PCs:

- PC1 (33% of variance): Captured variability primarily in fore-aft seat position (±55 mm in X, measured at mid-hip), spinal curvature (lumbar ±5°, thoracic ±11°), scapular protraction-

retraction (±15 mm in X, measured from the acromion (GH) to T4), anterior-posterior pelvic tilt (±6°), and head pitching (±6°) (Figure 7a).

- PC2 (23% of variance): Characterized by variations in lumbar spine curvature (±5°), anterior-posterior pelvic tilt (±9°), and head pitching (±7°). Additionally, steering input artifacts were present, as some volunteers were measured with a slight steering axle rotation (~6°), leading to fore-aft wrist position changes and corresponding elbow/shoulder angle adjustments (Figure 7b).
- PC3 (15% of variance): Represented asymmetrical sitting postures, with rotation around the superior-inferior axis and lateral displacement (±16 mm in Y, measured at mid-trochanter) (Figure 7c)
- PC4 (11% of variance): Primarily associated with scapular retraction-protraction (±13 mm in X, measured from the acromion (GH) to T4), along with minor elbow flexion-extension adjustments (±6°) (Figure 7d).

Figures and a qualitative description of all PCs' featured posture variation can be seen in Appendix B, whereas the quantitative difference in characteristic angles relative to the average posture is available in Appendix C.

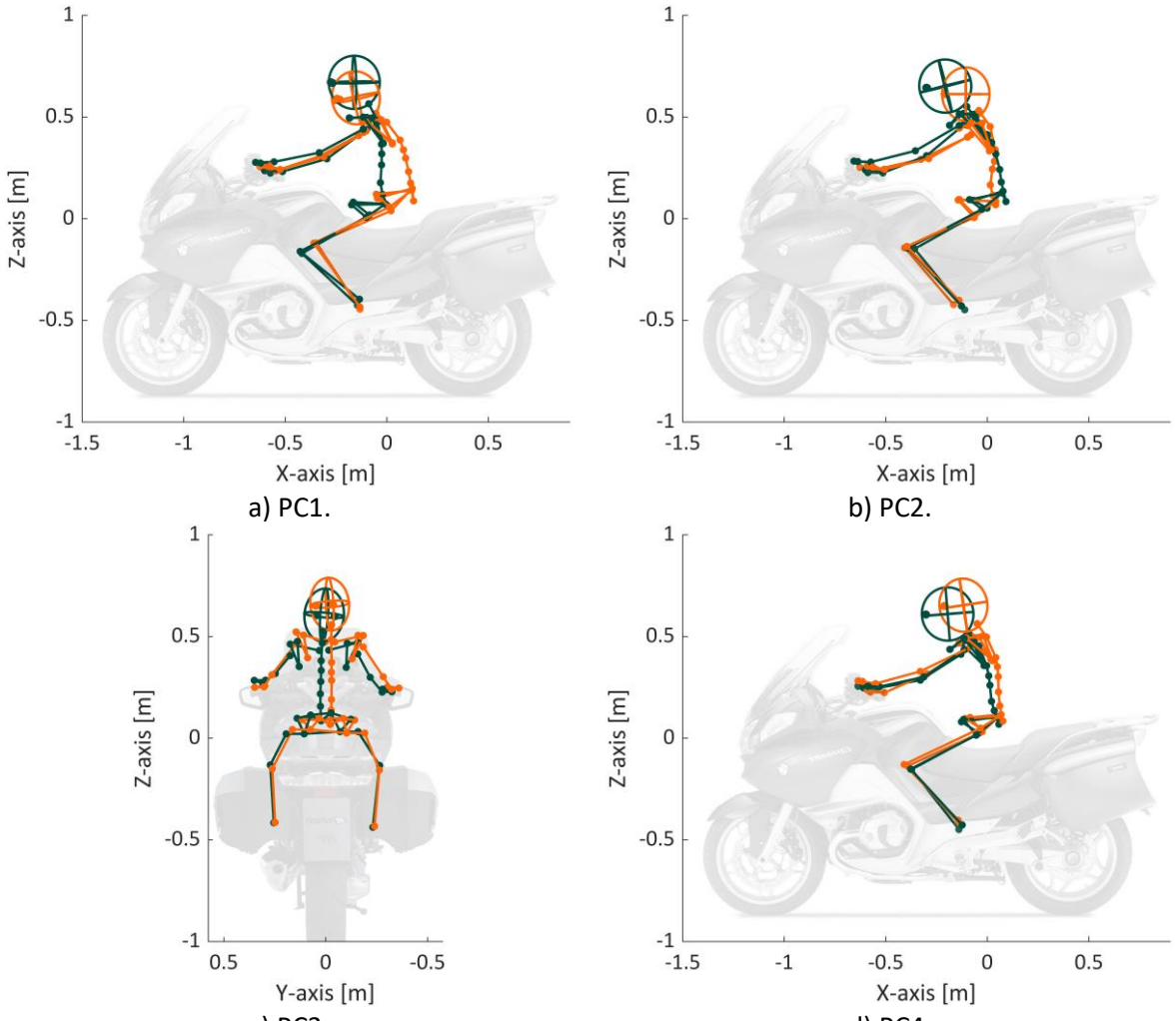

a) PC1. b) PC2.

c) PC3. d) PC4.

Figure 7. ±2 SD extreme postures of the first four PCs. Note: In this Figure, posture vs. PTW comparisons are unreliable due to non-comparable suspension travel and possible distortion effects. Background photo ©BMW Motorrad

3.2 Comparison with previously published male data

A comparison of the average riding posture for 50th percentile female and male riders is shown in Figure 8. On average, female riders sit 26 mm further forward on the saddle, with a smaller pelvis angle (14°), a larger hip mid-sagittal (MS) angle (13°), and a larger knee angle (10°). They also exhibit greater lower spine angles (6 to 9°) and the female's heads are on average positioned 35 mm lower to the MC than the males'. In contrast, the elbow, shoulder (MS and horizontal (H)), and upper spine angles remain similar between the two samples. Appendix C provides detailed characteristic angles for the female sample, while the corresponding male angles can be found in Lundin et al. (2024).

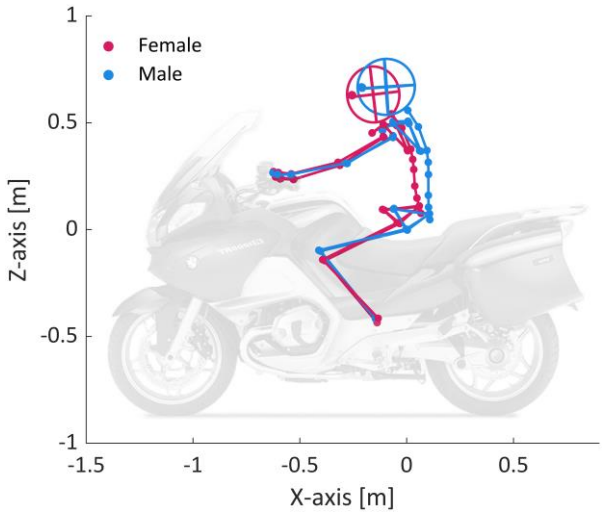

Figure 8. Comparison of average postures for the 50th percentile female sample(red) and the 50th percentile male sample (blue, data from Lundin et al. (2024)). Note: In this Figure, posture vs. PTW comparisons are unreliable due to non-comparable suspension travel and possible distortion effects. Background photo ©BMW Motorrad

Extending the analysis to include the ranges of characteristic angles, calculated across volunteers (Figure 9) highlights both differences and similarities between the male and female postures without any striking trends. Statistically significant differences ($p < 0.05$) were found for the hip (MS and H), pelvis, lumbar spine, and knee angles (Table 1).

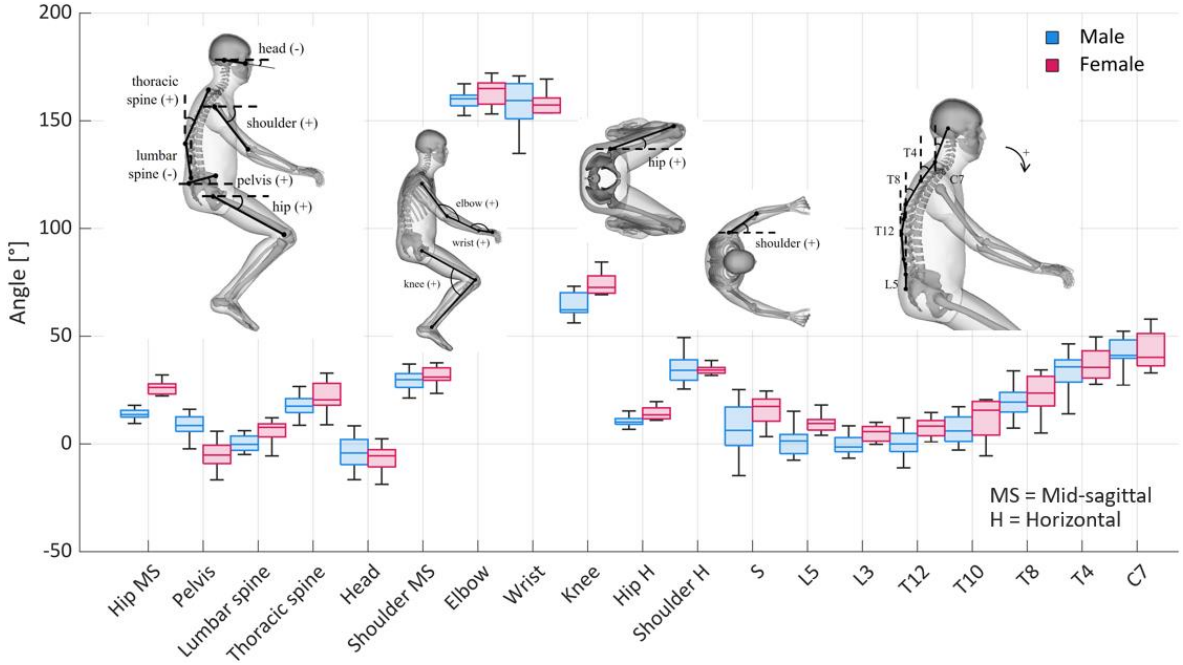

Figure 9. Box plot showing the distribution of characteristic angles for female and male samples.

Table 1. 95% confidence intervals for characteristic angles comparing female and male samples, with statistically significant angles shown in bold.

Characteristic angle	95% confidence interval
Hip MS	**-15.3 -10.2**
Pelvis	**8.3 19.3**
Lumbar spine	**-9.9 -2.1**
Thoracic spine	-10.0 1.2
Head	-2.8 8.0
Shoulder MS	-5.0 2.5
Elbow	-8.5 1.4
Wrist	-5.7 8.6
Knee	**-14.2 -5.8**
Hip H	**-6.3 -1.5**
Shoulder H	-3.7 3.3
S	**-19.6 -1.6**
L5	**-13.5 -5.5**
L3	-9.2 1.9
T12	-12.2 3.4
T10	-12.0 2.0
T8	-10.8 3.4
T4	-10.2 2.5
C7	-7.1 6.4

Comparing the first four PCs between the male and female datasets, reveals several commonalities and differences. Both groups exhibit variations in anterior-posterior pelvic tilt, fore-aft sitting

position, and knee flexion-extension, though the magnitude of these differences varies. Table 2 presents the ratio of maximum differences per angle between females and males for ±2SD extreme postures of the first PCs that explain 80% of the variance. Values > 1 indicate more pronounced variation in females, while values < 1 indicate more pronounced variation in males.

Notable spinal curvature differences were observed in both groups but were more pronounced in females (1.3 to 4 times greater), along with distinct differences in shape. Elbow flexion-extension (0.7), and angle variability in the horizontal plane for the hip (0.5) and shoulder (0.5), which was evident for the males, was less pronounced for the females. Conversely, scapular retraction-protraction were more apparent for the female than for the male PCs.

Table 2. Comparison of the maximum magnitudes of characteristic angles, as determined by the female-male quota, between ±2SD extreme postures within the first PCs explaining 80% of the variance.

Characteristic angle	**Max(±2SD PC 1-4 female)/Max(±2SD PC 1-7 male)**
Hip MS	1.0
Pelvis	1.2
Lumbar spine	1.5
Thoracic spine	1.7
Head	1.2
Shoulder MS	1.7
Elbow	0.7
Wrist	1.0
Knee	1.0
Hip H	0.5
Shoulder H	0.5
S	0.8
L5	1.7
L3	4.0
T12	3.5
T10	2.8
T8	1.6
T4	1.3
C7	0.9

4. Discussion

This study examined the preferred riding posture of ten 50th percentile females on a 2008 BMW R 1200 RT touring motorcycle based on photogrammetric measurements taken in a laboratory setup. The analysis provided both an average rider posture and common posture variations, identified through PCA. The first four PCs, explaining 81% of the total posture variability, were associated with fore-aft seat position, anterior-posterior pelvic tilt combined with spinal curvature and head position changes, scapular protraction and retraction, and asymmetrical seat positioning. These findings offer a data-driven representation of 50th percentile female rider postures, which can be applied in various contexts, including injury analysis in crash scenarios and safety system development.

Posture differences can influence rider kinematics in PTW crashes, particularly the common front-to-car side collisions, where head position can determine whether the head strikes the opposing vehicle in a crash or passes over it, leading instead to a thoracic-first impact (Langwieder, 1977; Schaper &

Grandel, 1985; Sporner et al., 1990). In this study, PC1, accounting for 33% of the total variability, captured a vertical head position difference of 76 mm (±2SD), likely accompanied by a substantial change in sternum angle due to altered thoracic spine curvature (22°, ±2SD). Such variations highlight the importance of incorporating diverse postures in crash simulations, particularly when assessing injury risks and might also influence rider interactions with protective devices such as PTW-mounted airbags.

One of the common features captured by the first two PCs relates to differences in anterior-posterior pelvic tilt. However, it is important to recognize that this variability may in part stem from individual differences in pelvic anatomy, affecting the relative distance and/or angle between the anterior and posterior superior iliac spine, rather than an actual change in tilt (Brynskog, 2025). Nonetheless, the postures identified in this study provide practical reference points for positioning 50th percentile female human surrogates for PTW safety assessments. The data, whether in the form of spatial marker positions (Appendices D, E, F) or associated angles (Appendix C), can be used to define postures for FE-HBMs using the *Landmark Positioning tool* available from v25.1.0. in the ANSA pre processor (BETA CAE Systems, Switzerland).

A comparison of characteristic angles suggests that 50th percentile female and male riders assume statistically different postures on touring motorcycles. This has implications for crash analysis, as using a single, common rider posture may not adequately represent both groups. The results suggest that human surrogates should incorporate anthropometrically driven posture differences, not only in terms of average postures but also to an extent in variability patterns (as described by the PCs). Moreover, the relatively small sample size in this study limits statistical power, making it difficult to detect more subtle differences which could possibly reveal further differences between the two groups.

The interquartile ranges of posture angles, presented in Figure 9, do not align with previous findings by Sabbah and Bubb (2008), which reported a greater variability in general among females compared to males in their sample. Instead, this study found that the degree of variability depended on the specific angle rather than being uniformly greater for females (Table 2).

Further research is needed to determine whether these observed differences between female and male postures hold across different PTW types. Step-through scooters, for example, may produce different posture trends due to their unique frame geometry and ergonomics. However, a scarcity of data exist on which PTWs are most used by female riders. Robertson and Minter (1996) found that, in a small self-reported study (n=31), touring motorcycles like the one used in this research were the most frequently ridden by female riders (36%). However, studies also suggest that L1 category vehicles (cylinder capacity ≤50 cm^3, max speed ≤50kph) may be more commonly used by females (ACEM, 2004), although the sample sizes remain limited. However, female PTW selection likely follows broader regional trends incorporating a variety of different types (Wisch et al., 2019), though physical constraints, such as seat height, may also play a role. Given that females, on average, have a shorter stature than males (Schneider et al., 1983), their choice of motorcycles is restricted by accessibility factors. The BMW R 1200 RT used in this study has a relatively low seat height (780 mm), making it more accessible for shorter riders despite being a large and heavy touring motorcycle (L3 vehicle).

An important question remains: do the observed posture differences in this study stem from sex, stature, or a combination thereof? While this study cannot directly answer that question, prior research, although lacking a direct comparison, suggests that rider posture is primarily influenced by stature rather than sex (Chou & Hsiao, 2005; Sabbah & Bubb, 2008). The significant differences

observed in pelvic, hip, and lumbar spine angles in this study suggest that shorter stature may lead 50th percentile female riders to adopt a more forward-leaning posture compared to their male counterpart. Given the restrictions on maximum forward position due to the fuel tank, this adjustment could be necessary to reach the handlebars. In turn, requiring compensatory changes in spine and hip angles, as well as a smaller head angle to maintain forward visibility and foot peg contact. These findings align with previous research by Sabbah and Bubb (2008), but it remains unclear whether males of similar stature would adopt comparable postures. Chou and Hsiao (2005) grouped riders by stature rather than sex and found that different height groups assumed distinct riding postures on step-through scooters, indicating that stature is a key factor also for PTWs lacking a restrictive fuel tank placement.

The methodology used in this study is further discussed in Lundin et al. (2024), including broader limitations applicable to both studies. A specific limitation in this dataset was that a few female participants were measured with a slight misalignment in the steering axis (~6°), inadvertently captured in the PCs as fore-aft hand movement and upper body compensation. While this feature was unintended, it highlights the challenges of recording postures in controlled laboratory environments, where certain real-world posture adjustments, such as those influenced by steering inputs, may not be fully replicated. Despite these limitations, the study provides valuable insights into 50th percentile female rider postures and their potential consequences for PTW crash analysis and safety system design.

Acknowledgements

The authors would like to thank Instituto de Biomecánica (IBV) for conducting the measurements. The Instituto de Biomecánica (IBV) is a R + D + i center where the behavior of the human body is studied and its relationship with the products, environments and services that people use. The authors would also like to acknowledge BMW Motorrad for supplying press photos of the touring MC.

References

ACEM. (2004). *MAIDS in-depth investigations of accidents involving powered two wheelers* (-). https://www.maids-study.eu/

Ariffin, A. H., Solah, M. S., Hamzah, A., Md Isa, M. H., Mohd Jawi, Z., Md Yusoff, N. I., & Hainin, M. R. (2016). Exploratory Study on Airbag Suitability for Low Engine Capacity Motorcycles. *Jurnal Teknologi*, *78*(4), 65-69. https://doi.org/10.11113/jt.v78.7999

Arunachalam, M., Mondal, C., Singh, G., & Karmakar, S. (2019). Motorcycle riding posture: A review. *Measurement*, *134*, 390-399. https://doi.org/10.1016/j.measurement.2018.10.019

Barbani, D., Baldanzini, N., & Pierini, M. (2014). Development and validation of an FE model for motorcycle-car crash test simulations. *International Journal of Crashworthiness*, *19*(3), 244-263. https://doi.org/10.1080/13588265.2013.874672

Barone, S., & Curcio, A. (2004). A computer-aided design-based system for posture analyses of motorcycles. *Journal of Engineering Design*, *15*(6), 581-595. https://doi.org/10.1080/09544820410001731146

Capitani, R., Pellari, S., & Lavezzi, R. (2010). Design and numerical evaluation on an airbag-jacket for motorcyclists. Int Conf. on ESAR, Hannover, Germany.

Chou, J.-R., & Hsiao, S.-W. (2005). An anthropometric measurement for developing an electric scooter. *International journal of industrial ergonomics*, *35*(11), 1047-1063. https://doi.org/10.1016/j.ergon.2005.06.001

Claflin, R. A. (2002). *Motorcycle rider posture prediction: The prediction of spinal curvature as a function of anthropometrics and point-of-contact chassis design* University of Central Florida]. Orlando (FL). https://search.proquest.com/openview/188c0857768205ecbabcbd0f02434ed9/1?pq-origsite=gscholar&cbl=18750&diss=y

ISO 13232-6 (2005). Motorcycles — Test and analysis procedures for research evaluation of rider crash protective devices fitted to motorcycles — Part 6: Full-scale impact-test procedures. In.

Langwieder, K. (1977, October). Collision characteristics and injuries to motorcyclists and moped drivers. Stapp Car Crash Conference, New Orleans, Louisiana, USA.

Lundin, L., Oikonomou, M., Lioras, A., Mihailidis, A., Pipkorn, B., Rorris, L., Svensson, M. Y., & Iraeus, J. (2024). Quantifying rider posture variability in powered two-and three-wheelers for safety assessment. *Traffic Injury Prevention*, 1-12. https://doi.org/10.1080/15389588.2024.2351607

Maier, S., Doléac, L., Hertneck, H., Stahlschmidt, S., & Fehr, J. (2021). Finite element simulations of motorcyclist interaction with a novel passive safety concept for motorcycles. IRCOBI Conference, Online.

Maier, S., & Fehr, J. (2023). Efficient simulation strategy to design a safer motorcycle. *Multibody System Dynamics*, 1-28. https://doi.org/10.1007/s11044-023-09879-8

Maier, S., Kempter, F., Kronwitter, S., & Fehr, J. (2022). Positioning and Simulation of Human Body Models on a Motorcycle with a Novel Restraint System. IRCOBI Conference, Porto, Portugal.

MATLAB Statistics and Machine Learning Toolbox. In. (2023). (Version R2023b) [software]. The MathWorks Inc.

Prochowski, L., & Pusty, T. (2013). Analysis of motorcyclist's body movement during a motorcycle impact against a motor car side. *Journal of KONES powertrain and transport*, *20*(4), 371-379. https://doi.org/10.5604/12314005.1137849

Robertson, S., & Minter, A. (1996). A study of some anthropometric characteristics of motorcycle riders. *Applied Ergonomics*, *27*(4), 223-229.

Rogers, N. M., & Zellner, J. W. (2001). Factors and status of motorcycle airbag feasibility research. ESV Conference, Amsterdam, Netherlands.

Sabbah, A. O., & Bubb, H. (2008). Development of a motorcycle posture model for DHM systems. Digital Human Modeling for Design and Engineering Symposium, Pittsburgh (PA).

Schaper, D., & Grandel, J. (1985). Motorcycle Collisions with Passenger Cars — Analysis of Impact Mechanism, Kinematics, and Effectiveness of Full Face Safety Helmets [Conference Paper]. *SAE Transactions 94*, *94*(Section 1), 544-551. https://doi.org/10.4271/850094

Schneider, L. W., Robbins, D. H., Pflüg, M. A., & Snyder, R. G. (1983). *Development of anthropometrically based design specifications for an advanced adult anthropomorphic dummy family, volume 1. final report* (UMTRI-83-53-1). https://deepblue.lib.umich.edu/bitstream/handle/2027.42/259/72268.0001.001.pdf

Smith, T., Zellner, J., & Rogers, N. M. (2006). A three dimensional analysis of riding posture on three different styles of motorcycle. International Motorcycle Safety Conference, Long Beach (CA).

Sporner, A., Langwieder, K., & Polauke, J. (1990). Passive Safety for Motorcyclists—from the Legprotector to the Airbag. *JOURNAL OF PASSENGER CARS*, *99*(Section 6), 1064-1073. https://doi.org/10.4271/900756

Van Auken, R. M., Kebschull, S. A., Broen, P. C., Zellner, J. W., & Rogers, N. M. (2005). Development of a Rider Size and Position Model to Determine Motorcycle Protective Device Test Conditions. ESV Conference, Washington (DC).

WHO. (2023). *Global status report on road safety 2023*. https://www.who.int/publications/i/item/9789240086517

Wisch, M., Breunig, S., Piantini, S., Schick, S., Whyte, T., Brown, J., Canu, A., Perrin, C., Serre, T., Perera, N., Martínez, E., Tobar, M., Ferrer, A., & Pieve, M. (2019). PIONEERS Deliverable D1.1 Powered Two-Wheelers–Road Traffic Accident Scenarios and Common Injuries (1.1). https://pioneers-project.eu/wp-content/uploads/2020/12/Deliverable-D1.1.pdf

Appendix A – Volunteer anthropometry

Table A1 Volunteer height and weight for the two measurement sessions.

	Session 1		Session 2	
Volunteer	Height [cm]	Weight [kg]	Height [cm]	Weight [kg]
1	158.2	59.1	158.1	58.0
2	163.2	63.7	163.1	63.4
3	168.0	57.0	168.5	57.0
4	163.1	56.4	162.7	56.1
5	158.0	63.0	157.6	64.0
6	160.8	67.0	160.5	65.2
7	163.0	60.4	162.6	59.9
8	167.4	58.2	166.5	56.2
9	163.7	67.0	163.4	67.3
10	164.8	60.2	164.0	59.5

Appendix B: Posture features of PCs

Table B1 Textual and visual description of the ±2 SD postural features along the nine principal components (PCs). The PTW background image is for illustration purposes. Note: In these Figures, posture vs. PTW comparisons are unreliable due to non-comparable suspension travel and possible distortion effects. Background photo ©BMW Motorrad

<table>
<tr><td>PC #</td><td colspan="2">Characterized variation & Figures of PC postural features relative average, -2 SD extreme posture in dark green and +2SD in orange.</td></tr>
<tr><td rowspan="2">1
33%</td><td>More pronounced:
Fore-aft sitting pos
Curved-straight spine
Protraction-retraction scapulae
Anterior-posterior pelvic tilt
Pitching head</td><td>Less pronounced:
Flexion-extension knee
Flexion-extension wrist</td></tr>
<tr><td colspan="2"> 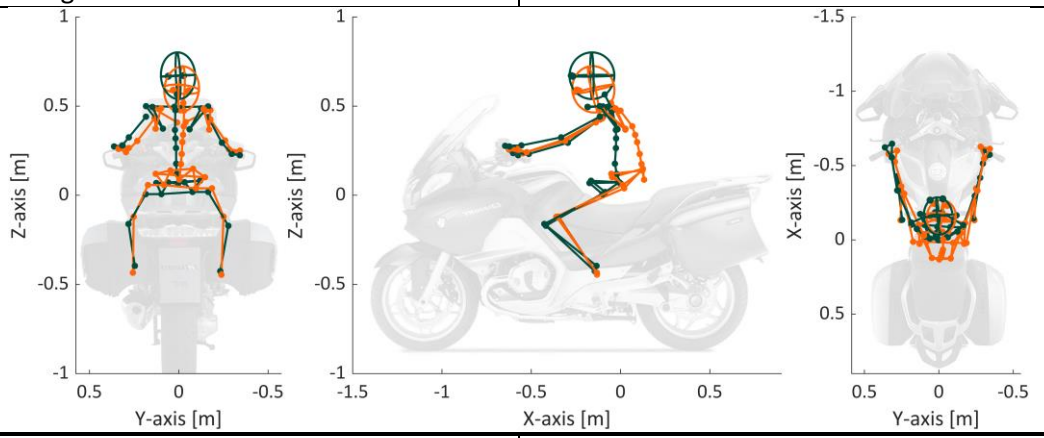
</td></tr>
<tr><td rowspan="2">2
23%</td><td>More pronounced:
Steering input (from measurement error)
Curved-straight spine
Pitching head
Anterior-posterior pelvic tilt</td><td>Less pronounced:
Fore-aft sitting pos
LHS-RHS sitting position
Flexion-extension shoulder</td></tr>
<tr><td colspan="2"> 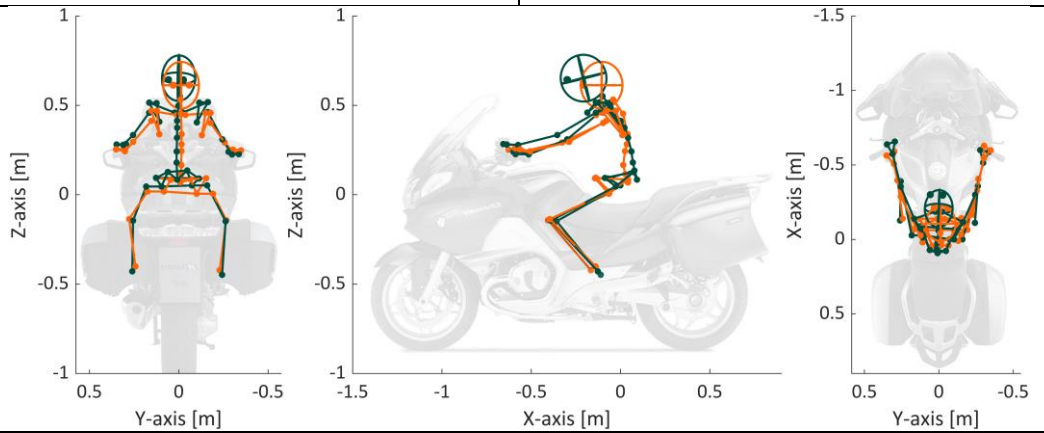
</td></tr>
<tr><td>3
15%</td><td>More pronounced:
LHS-RHS twist (rotation superior-inferior axis)
LHS-RHS sitting position</td><td>Less pronounced:
Flexion-extension elbow
Flexion-extension shoulder</td></tr>
</table>

	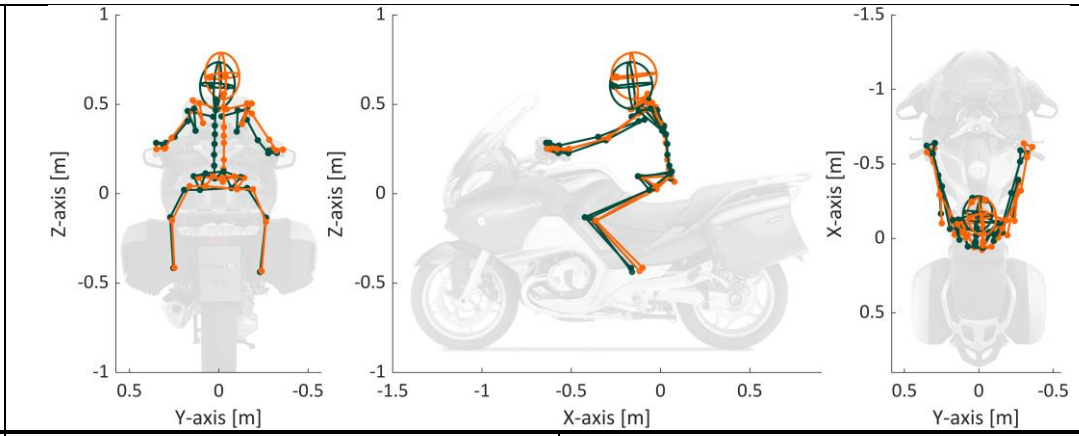	
4 11%	**More pronounced:** Protraction-retraction scapulae	**Less pronounced:** Flexion-extension elbow Fore-aft sitting position
	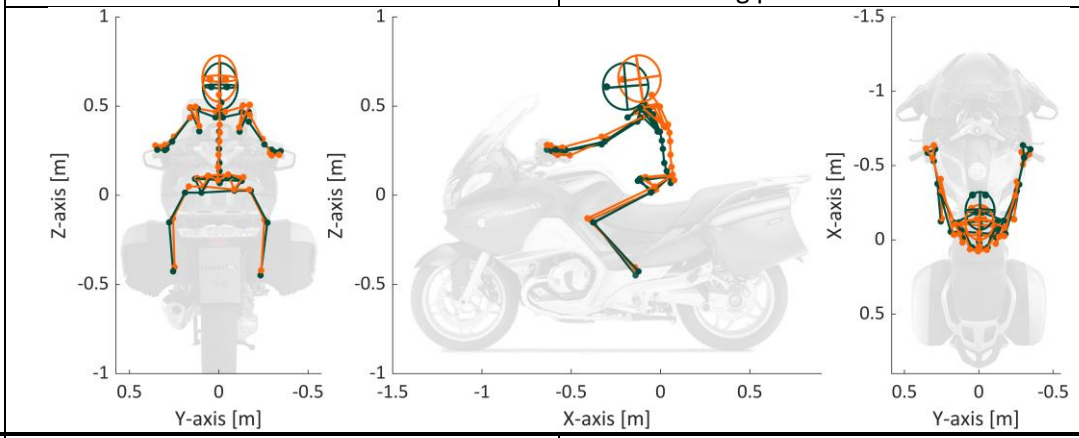	
5 7%	**More pronounced:** Pitching head Raised-lowered shoulders	**Less pronounced:** Flexion-extension knee Flexion-extension wrist Anterior-posterior pelvic tilt
	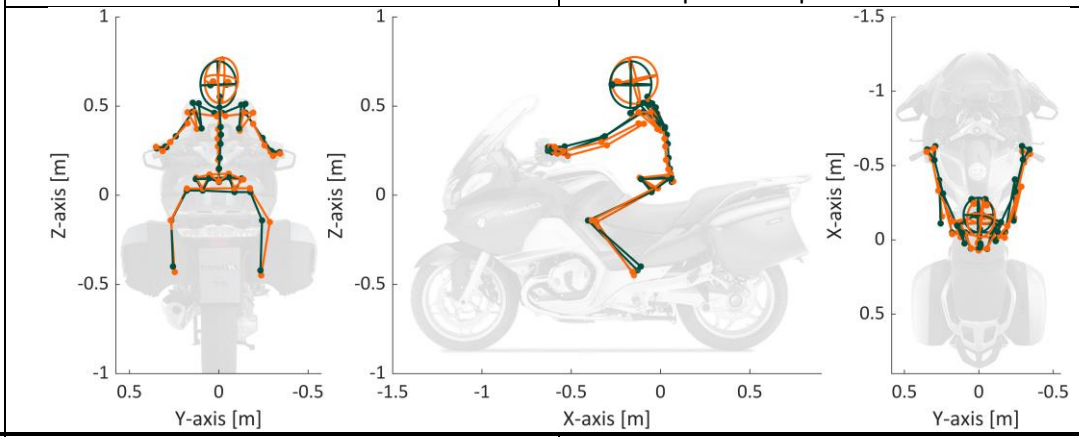	
6 4%	**More pronounced:** Size/shape pelvis Abduction-adduction hip	**Less pronounced:** Curved-straight lumbar spine

	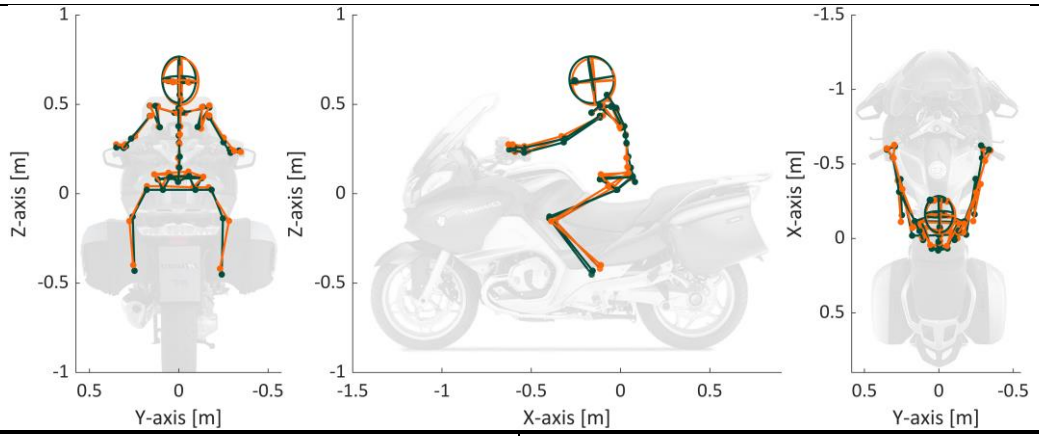	
7 3%	**More pronounced:** Anterior-posterior pelvic tilt	**Less pronounced:**
	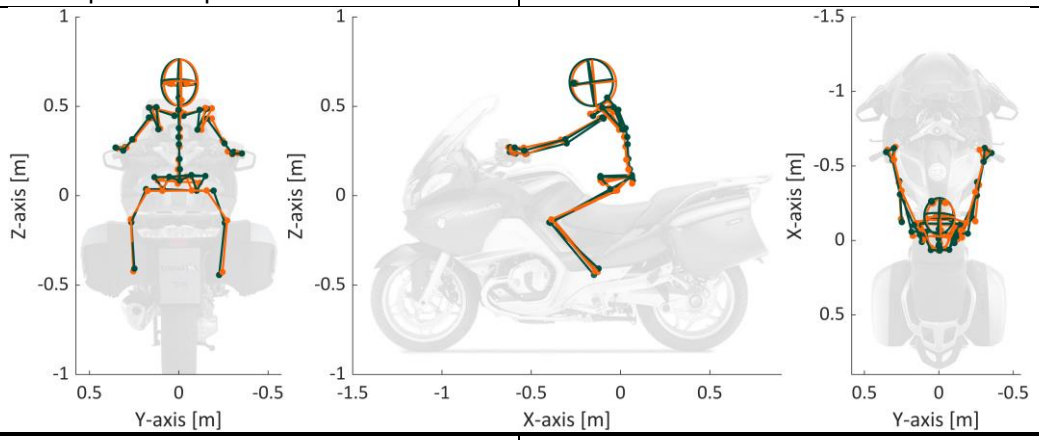	
8 3%	**More pronounced:**	**Less pronounced:** Protraction-retraction shoulders Anterior-posterior pelvic tilt Size/shape pelvis
	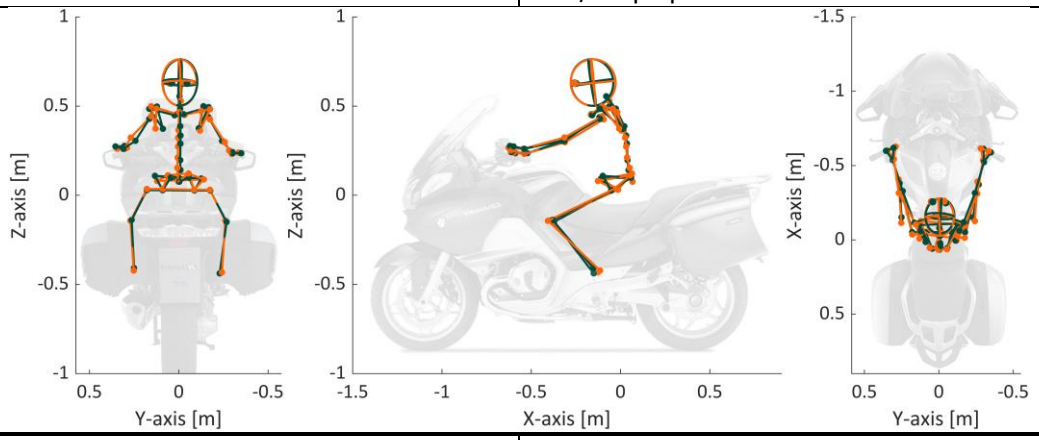	
9 2%	**More pronounced:**	**Less pronounced:** Flexion-extension wrist Pitching head

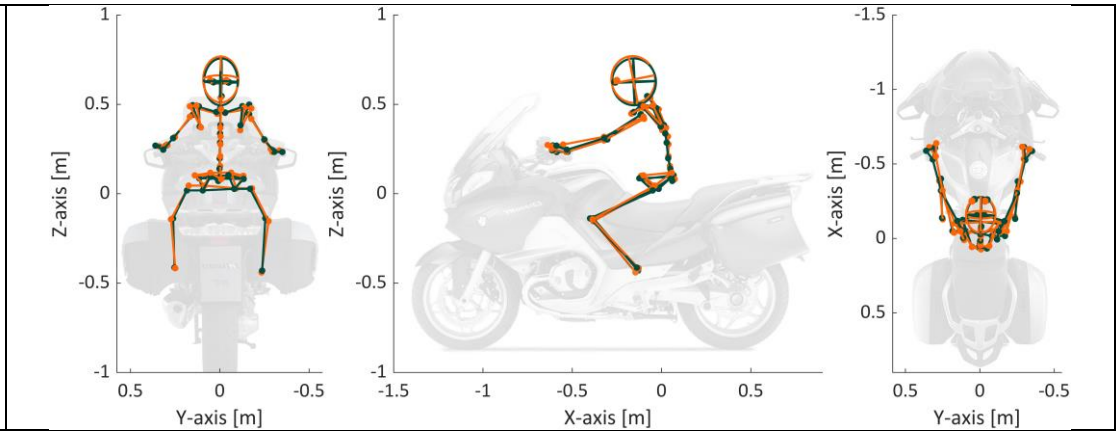
Z-axis [m]
Y-axis [m]
Z-axis [m]
X-axis [m]
X-axis [m]
Y-axis [m]

Appendix C: Characteristic angles for ±2 SD PC extreme postures

Table C1. Characteristic angles for average posture and ±difference corresponding to ±2 SD extreme postures for each PC. Description of the characteristic angles are available in Lundin et al. (2024). MS=mid-sagittal plane, H=horizontal plane.

Angles	Average	PC1	PC2	PC3	PC4	PC5	PC6	PC7	PC8	PC9
Head	-6.7	5.7	7.2	0.7	1.9	6.7	2.6	1.6	1.8	4.4
Pelvis	-5.2	5.9	8.5	2.6	0.4	3.4	1.5	4.2	5.8	0.4
Shoulder LHS MS	32.4	4.0	7.2	4.2	0.1	2.2	1.8	1.5	1.6	4.3
Shoulder RHS MS	29.8	1.6	0.4	8.4	4.2	2.8	3.1	0.8	0.2	2.9
Hip LHS MS	26.5	3.1	2.9	1.1	1.8	2.4	3.5	1.0	2.1	2.4
Hip RHS MS	26.3	0.9	1.5	3.4	0.9	0.9	5.0	2.2	0.6	2.2
Shoulder LHS H	31.3	3.4	4.0	2.9	3.4	3.2	1.5	4.8	1.6	0.4
Shoulder RHS H	38.4	1.1	2.6	1.1	1.7	4.0	1.2	0.9	5.8	1.7
Hip LHS H	14.2	4.4	2.0	2.5	1.2	3.8	4.9	3.9	1.5	1.1
Hip RHS H	14.2	2.2	2.8	2.0	1.1	0.3	2.7	0.6	0.3	1.8
Wrist LHS	157.1	8.5	3.8	2.0	6.4	5.3	3.3	5.5	3.7	3.5
Wrist RHS	159.9	11.6	3.5	4.6	4.2	12.7	1.7	9.4	2.6	14.1
Knee LHS	75.8	4.3	3.7	1.2	3.2	6.3	0.4	1.2	4.0	2.5
Knee RHS	72.8	7.2	2.6	2.1	1.4	5.7	0.1	1.1	3.6	2.0
Elbow LHS	164.3	4.0	2.5	7.3	7.0	0.9	4.7	5.6	0.7	3.9
Elbow RHS	162.4	2.3	1.3	9.2	6.4	0.5	6.0	0.3	2.5	0.3
S	14.9	7.1	2.0	8.4	3.3	7.1	1.9	0.4	3.6	5.6
L5	10.0	0.2	2.9	0.4	5.7	3.6	3.1	1.6	4.1	1.8
L3	3.4	8.1	10.7	1.9	2.4	0.1	4.4	0.7	1.5	2.7
T12	5.9	8.2	17.4	2.1	0.9	0.3	0.9	2.4	0.3	2.6
T10	10.8	8.3	16.5	1.7	1.2	2.6	4.2	0.2	0.1	1.7
T8	22.9	14.0	11.4	0.6	1.5	2.4	1.2	1.4	3.0	1.2
T4	36.7	11.8	1.3	4.5	1.5	1.4	0.8	7.1	1.2	0.9
Lumbar spine	6.2	4.9	5.1	0.7	3.4	1.5	4.0	1.1	3.0	2.1
Thoracic spine	22.0	10.9	9.2	1.4	0.2	1.5	0.3	1.9	1.7	0.8
C7	43.1	9.1	4.1	6.5	5.9	10.1	2.0	3.0	2.3	0.3

Appendix D: Marker position for average posture

Table D1 Spatial marker coordinates for average postures corresponding to μ from the PCA. Marker description available in Lundin et al. (2024).

Markers	X [mm]	Y [mm]	Z [mm]
ASIS_l	1115.5	225.8	1017.6
ASIS_r	1108.5	486.1	1020.7
C7	1150.0	351.1	1467.8
clv_l	1060.2	328.8	1379.1
clv_r	1059.7	375.8	1378.5
fi2_r	598.1	655.9	1197.5
fi2_l	607.5	67.6	1172.8
fi5_r	621.1	708.5	1193.4
fi5_l	628.6	16.5	1163.7
gh_l	1115.0	188.0	1414.3
gh_r	1112.0	518.4	1418.4
L3	944.8	514.2	1750.3
L5	1184.3	543.9	1702.4
lc_l	1203.1	146.4	1665.0
lc_r	930.3	182.8	1736.2
le_l	1259.4	357.6	1130.4
le_r	1269.4	358.4	1073.7
lm_l	852.6	57.2	790.4
lm_r	838.2	657.2	794.1
o	902.7	91.8	1247.3
ob_l	897.2	629.5	1264.6
ob_r	1100.4	105.8	489.5
PSIS_l	1106.0	629.4	514.0
PSIS_r	1185.4	352.2	1580.3
rs_l	977.8	325.3	1548.5
rs_r	979.6	384.6	1548.5
si_l	1280.4	302.6	1037.2
si_r	1278.2	411.6	1031.8
ss_l	685.0	79.5	1163.9
ss_r	675.2	642.6	1188.1
T10	1226.4	243.4	1295.3
T12	1224.5	467.8	1299.8
T4	1176.2	226.7	1412.0
T8	1170.8	482.4	1417.4
t_l	1250.0	355.8	1255.0
t_r	1254.9	356.2	1207.6
tr_l	1199.0	353.8	1402.0
tr_r	1240.9	355.3	1302.8
us_l	1188.9	183.4	954.9
us_r	1177.3	537.4	958.3
me_r	1066.6	256.1	1558.0
mc_r	1063.5	449.3	1559.2

mm_r	698.3	37.4	1156.4
me_l	686.8	687.1	1185.8
mc_l	903.0	599.7	1217.3
mm_l	818.2	594.3	777.2
S	1070.2	590.9	508.7

Appendix E: Principal component loadings

Table E1 Principal component loadings. Marker description available in Lundin et al. (2024).

Markers [X; Y; Z] [mm]	**PC1**	**PC2**	**PC3**	**PC4**
asicl	186.3; -44.4; 30.4	-139.9; -75.4; 2.9	-12.1; -43.3; -9.3	115.4; -25.2; 58.4
asicr	191.0; 5.0; 81.7	-95.8; 0.9; 1.9	64.7; -60.3; -16.2	23.9; -31.2; 12.2
c7	54.9; -56.3; -73.7	111.7; -8.4; -36.8	-10.5; -100.8; 79.8	116.9; 37.9; 116.3
clvl	67.0; -27.3; -131.7	92.4; -29.2; -24.1	-30.2; -70.6; 94.6	120.2; -32.0; 85.9
clvr	73.1; -23.9; -137.5	91.4; -25.3; -26.1	-2.6; -68.2; 99.6	122.4; -5.5; 83.9
fi2r	72.0; -53.0; -18.6	126.5; 7.4; -45.7	79.5; 8.2; -64.1	-68.8; 23.0; 60.5
fi2l	-39.1; 30.7; 32.8	-53.7; -47.9; 23.5	-107.5; -54.0; 26.6	122.0; 26.6; -48.5
fi5r	67.8; -39.0; -21.5	140.3; 6.1; -52.0	102.5; -4.0; -81.6	-77.2; 29.2; 65.4
fi5l	-61.3; -2.4; 40.3	-19.2; -23.4; 38.8	-98.6; -81.0; 42.8	92.3; 22.7; -56.6
ghl	-23.3; -20.7; -31.5	34.5; -27.9; -113.5	-75.4; -63.5; 81.0	125.4; -17.2; 105.8
ghr	21.8; -75.1; -24.5	109.8; -22.6; -86.4	61.7; -68.3; 139.1	27.4; -2.6; 8.7
h1	0.4; -74.5; -85.8	189.7; -4.1; -80.4	-73.8; 27.8; -5.2	162.2; 31.8; 84.4
h2	-15.8; -43.3; -98.1	237.7; -31.2; -98.1	-19.8; -55.2; 161.1	179.5; -17.8; 155.6
h3	7.9; -50.2; -164.0	206.2; -9.3; -80.7	-62.8; -64.0; 296.1	117.6; -8.1; 162.7
h4	16.9; -67.5; -144.6	171.3; 6.5; -43.7	-121.4; 15.0; 91.9	111.4; 35.4; 72.1

l3	217.8; -49.1; 85.0	-86.8; -49.0; -143.8	-2.6; -129.0; -65.3	93.1; 12.9; 124.4
l5	218.1; -36.8; 86.6	-79.5; -48.3; -122.7	-4.5; -123.7; -44.3	73.4; 20.1; 63.1
lcl	83.8; 51.0; 82.7	-70.0; -26.5; 6.5	51.7; -20.2; -55.0	-68.3; 23.8; 13.5
lcr	71.9; -74.4; 62.8	15.3; 63.3; 30.0	175.2; 22.9; -36.2	-100.3; -45.6; 53.3
lel	-58.3; -0.5; 16.8	-43.1; -3.5; -28.0	-47.5; -150.3; 12.5	75.4; -7.2; 76.1
ler	41.7; -70.4; -33.7	124.6; 7.1; -74.7	129.6; 43.7; -19.1	-43.4; -34.3; 120.7
lml	16.8; 9.2; -23.4	-100.0; 10.7; 37.9	106.4; -38.5; 34.6	30.8; -19.2; 106.1
lmr	6.9; -14.8; -45.8	-22.3; -29.3; 50.7	167.7; -11.0; 20.0	-46.8; -0.5; 77.1
o	1.2; -29.1; -124.3	169.1; -30.1; -75.1	40.5; -83.7; 216.6	179.2; -9.5; 151.1
obl	15.1; -49.8; -151.5	163.3; -10.8; -38.0	9.9; -40.9; 116.9	175.6; 50.7; 98.3
obr	3.1; -36.1; -142.1	181.1; -8.9; -31.7	19.4; -56.6; 117.8	188.5; 47.9; 98.4
psicl	206.8; -74.6; 119.2	-70.2; -33.4; -93.0	-18.3; -141.6; -63.7	48.0; 15.6; 29.2
psicr	205.6; -19.4; 105.4	-56.1; -31.3; -81.6	11.8; -98.0; -39.4	36.6; 37.4; 24.6
rsl	-37.5; -3.4; -2.7	-66.6; -12.1; 29.3	-55.5; -113.6; 36.1	139.4; 23.8; -47.6
rsr	60.0; -32.3; -55.8	121.1; -15.9; -59.9	138.3; -12.1; -40.6	-52.4; 19.8; 45.2
sil	68.8; -172.6; -2.8	19.1; -52.7; -134.3	-51.7; -69.8; 99.7	115.5; 7.4; 65.0
sir	75.2; 64.3; -0.9	61.4; 0.2; -132.3	-28.8; -99.0; 101.2	79.1; 0.4; 79.7

ssl	33.2; -22.7; -5.4	48.7; -65.5; -110.6	-96.3; -123.1; 91.8	135.1; -15.9; 98.4
ssr	72.1; -76.3; -13.8	91.0; -3.3; -82.2	24.8; -71.5; 73.1	63.1; 34.1; 31.0
t10	166.9; -65.4; 30.6	25.9; -45.2; -174.1	-7.2; -117.5; -19.3	114.4; -15.8; 121.3
t12	185.9; -55.0; 51.7	-31.6; -46.1; -140.9	-18.6; -124.5; 13.4	111.1; -5.3; 114.7
t4	68.7; -74.8; -5.1	138.8; -26.9; -84.7	-19.5; -103.0; 41.2	101.6; 6.5; 117.7
t8	143.8; -77.3; 32.7	73.9; -47.7; -140.5	-0.2; -120.8; -18.9	122.7; -7.4; 108.0
tl	166.3; -33.4; 32.6	-120.2; -62.3; -87.9	48.5; -76.3; -16.4	41.8; 24.0; 17.1
tr	179.2; -19.2; 79.5	-64.5; -13.7; -53.1	89.8; -71.5; 49.2	56.4; -57.0; 92.7
trl	36.9; -32.9; -135.6	187.1; -37.7; -68.3	11.4; -60.0; 159.5	215.8; 16.2; 117.4
trr	-12.3; -29.7; -102.9	194.7; -13.5; -80.0	65.9; -67.3; 90.7	204.3; 7.3; 116.9
usl	-64.6; -20.6; 15.3	-52.3; -3.8; 34.8	-77.5; -102.2; 31.8	116.6; 18.5; -60.8
usr	34.1; -34.6; -61.6	129.7; -19.0; -74.2	129.5; -14.1; -40.3	-54.6; 26.5; 34.8
mer	28.0; -77.2; -29.8	123.0; -8.0; -70.8	135.2; 34.0; -12.6	-51.6; -17.1; 27.7
mcr	138.7; -16.3; 64.0	-36.7; 18.6; 2.5	111.8; -69.2; -51.5	-70.4; -69.9; 69.6
mmr	-1.0; 49.0; -72.7	-24.2; -37.9; 51.9	137.2; -18.6; -11.9	-59.9; -45.2; 51.0
mel	-54.1; -55.6; 24.2	-64.0; -45.6; -38.4	-25.3; -150.2; 1.3	104.8; 65.7; 92.7
mcl	142.7; 33.5; 77.9	-111.8; 14.3; 15.5	51.7; 25.0; -50.0	-37.1; 63.7; 75.2

mml	23.8; -29.0; -40.0	-107.6; 41.6; 58.7	90.2; -2.5; -12.2	-18.4; -0.3; 40.2
s	203.3; -10.7; 35.1	-95.1; -31.5; -30.4	47.8; -105.6; -42.9	55.2; 27.0; 43.5

Appendix F: Standard deviation of PC scores

Table F1 Standard deviations (SDs) of the first four principal component scores.

PC #	SD
1	0.160
2	0.132
3	0.106
4	0.0924